

Prompt $\Upsilon(nS)$ production at the LHC in the Regge limit of QCD

M.A. Nefedov,^{*} V.A. Saleev,[†] and A.V. Shipilova[‡]

Samara State University, Academic Pavlov Street 1, 443011 Samara, Russia

Abstract

We study prompt $\Upsilon(nS)$ hadroproduction ($n = 1, 2, 3$) invoking the hypothesis of gluon Reggeization in t -channel exchanges at high energy and the factorization formalism of nonrelativistic quantum chromodynamics at leading order in the strong-coupling constant α_s and the relative velocity v of the bound quarks. The transverse-momentum distributions of prompt $\Upsilon(nS)$ -meson production measured by the ATLAS Collaboration at the CERN LHC are fitted to obtain the color-octet nonperturbative long-distance matrix elements, which are used to predict prompt $\Upsilon(nS)$ production spectra measured by the CMS and LHCb Collaborations. At the numerical calculation, we adopt the Kimber-Martin-Ryskin prescription to derive unintegrated gluon distribution function of the proton from its collinear counterpart, for which we use the Martin-Roberts-Stirling-Thorne set. We find good agreement with measurements by the ATLAS, CMS and LHCb Collaborations at the LHC at the hadronic c.m. energy $\sqrt{S} = 7$ TeV as well as with measurements by the CDF Collaboration at the Fermilab Tevatron.

PACS numbers: 12.38.-t,12.40.Nn,13.85.Ni,14.40.Gx

^{*}Electronic address: nefedovma@gmail.com

[†]Electronic address: saleev@samsu.ru

[‡]Electronic address: alexshipilova@samsu.ru

I. INTRODUCTION

The production of charmonium and bottomonium states at hadron colliders has provided a useful laboratory for testing the high-energy limit of quantum chromodynamics (QCD) as well as the interplay of perturbative and nonperturbative phenomena in QCD. The additional interest to heavy quarkonium production is motivated by the idea that it can be distinguished as a signal manifesting new phenomena, such as quark-gluon plasma production, color-transparency, associated Higgs boson production and so on. The experimental study of bottomonium production at the Large Hadron Collider (LHC) is included in programs of main CERN Collaborations: ATLAS [1], CMS [2], and LHCb [3].

The total collision energies, $\sqrt{S} = 7$ TeV or 14 TeV at the LHC, sufficiently exceed the characteristic scale μ of the relevant hard processes, which is of order of quarkonium transverse mass $M_T = \sqrt{M^2 + p_T^2}$, *i.e.* we have $\Lambda_{\text{QCD}} \ll \mu \ll \sqrt{S}$. In this high-energy regime, so called "Regge limit", the contribution of partonic subprocesses involving t -channel parton (gluon or quark) exchanges to the production cross section can become dominant. Then the transverse momenta of the incoming partons and their off-shell properties can no longer be neglected, and we deal with "Reggeized" t -channel partons. These t -channel exchanges obey multi-Regge kinematics (MRK), when the particles produced in the collision are strongly separated in rapidity. If the same situation is realized with groups of particles, then quasimulti-Regge kinematics (QMRK) is at work. In the case of $\Upsilon(nS)$ -meson inclusive production, this means the following: $\Upsilon(nS)$ -meson (MRK) or $\Upsilon(nS)$ -meson plus gluon jet (QMRK) are produced in the central region of rapidity, while other particles are produced with large modula of rapidities.

The parton Reggeization approach [4, 5] is particularly appropriate for high-energy phenomenology. We see, the assumption of a dominant role of MRK or QMRK production mechanisms at high energy works well. The parton Reggeization approach is based on an effective quantum field theory implemented with the non-Abelian gauge-invariant action including fields of Reggeized gluons [6] and Reggeized quarks [7]. Reggeized partons interact with quarks and Yang-Mills gluons in a specific way. Recently, in Ref.[8], the Feynman rules for the effective theory of Reggeized gluons were derived for the induced and some important effective vertices. This approach was successfully applied to interpret the production of isolated jets [9], dijet azimuthal decorrelations [10], prompt photons [11], diphotons [12],

charmed mesons [13], bottom-flavored jets [14], Drell-Yan lepton pairs [15] measured at the Fermilab Tevatron, at the DESY HERA and at the CERN LHC, especially in the small- p_T regime, where $p_T \ll \sqrt{S}$.

We suggest the MRK or QMRK production mechanisms to be dominant also for heavy-quarkonium production at the LHC. Using the Feynman rules [8] for the effective theory, we can construct heavy-quarkonium production amplitudes in the non-relativistic QCD (NRQCD)[16, 17]. The factorization formalism of the NRQCD is a rigorous theoretical framework for the description of heavy-quarkonium production and decay. The factorization hypothesis of NRQCD assumes the separation of the effects of long and short distances in heavy-quarkonium production. NRQCD is organized as a perturbative expansion in two small parameters, the strong-coupling constant α_s and the relative velocity v of the heavy quarks inside a heavy quarkonium.

Our previous analysis of charmonium [18, 19] and bottomonium [19, 21] production at the Fermilab Tevatron and charmonium production [20] at the CERN LHC using the high-energy factorization scheme and the NRQCD approach has shown the efficiency of such type of high-energy phenomenology. In this paper we perform calculations for the prompt $\Upsilon(nS)$ -meson transverse momentum spectra at the CERN LHC to obtain color-octet nonperturbative matrix elements (NMEs) by fitting procedure using experimental data from the ATLAS Collaboration [1]. Then we predict prompt $\Upsilon(nS)$ -meson spectra, which were measured recently by the CMS [2] and LHCb [3] CERN LHC Collaborations at the energy of $\sqrt{S} = 7$ TeV and a few years before by the CDF [22] Fermilab Tevatron Collaboration at the energy of $\sqrt{S} = 1.8$ TeV. We find a good agreement of our calculations and experimental data.

II. MODEL

Working at the leading order (LO) in α_s and v we consider the following partonic subprocesses, which describe bottomonium production at high energy:

$$R(q_1) + R(q_2) \rightarrow \mathcal{H}[{}^3P_J^{(1)}, {}^3S_1^{(8)}, {}^1S_0^{(8)}, {}^3P_J^{(8)}](p), \quad (1)$$

$$R(q_1) + R(q_2) \rightarrow \mathcal{H}[{}^3S_1^{(1)}](p) + g(p'), \quad (2)$$

where R is a Reggeized gluon and g is an on-shell Yang-Mills gluon, respectively, with four-momenta indicated in parentheses, $\mathcal{H}[n]$ is a physical bottomonium state, $n = {}^{2S+1}L_J^{(1,8)}$ is a

$b\bar{b}$ Fock state with a spin S , total angular momentum J , orbital angular momentum L and with the color-singlet (1) or the color-octet (8) quantum numbers.

In the general case, the partonic cross section of bottomonium production receives from the $b\bar{b}$ Fock state $[n] = [^{2S+1}L_J^{(1,8)}]$ the contribution [16, 17]

$$d\hat{\sigma}(R + R \rightarrow b\bar{b}[^{2S+1}L_J^{(1,8)}] \rightarrow \mathcal{H}) = d\hat{\sigma}(R + R \rightarrow b\bar{b}[^{2S+1}L_J^{(1,8)}]) \frac{\langle \mathcal{O}^{\mathcal{H}}[^{2S+1}L_J^{(1,8)}] \rangle}{N_{\text{col}} N_{\text{pol}}}, \quad (3)$$

where $N_{\text{col}} = 2N_c$ for the color-singlet state, $N_{\text{col}} = N_c^2 - 1$ for the color-octet state, and $N_{\text{pol}} = 2J + 1$, $\langle \mathcal{O}^{\mathcal{H}}[^{2S+1}L_J^{(1,8)}] \rangle$ are the NMEs. They satisfy the multiplicity relations

$$\begin{aligned} \langle \mathcal{O}^{\psi(nS)}[{}^3P_J^{(8)}] \rangle &= (2J + 1) \langle \mathcal{O}^{\psi(nS)}[{}^3P_0^{(8)}] \rangle, \\ \langle \mathcal{O}^{\chi_{cJ}}[{}^3P_J^{(1)}] \rangle &= (2J + 1) \langle \mathcal{O}^{\chi_{c0}}[{}^3P_0^{(1)}] \rangle, \\ \langle \mathcal{O}^{\chi_{cJ}}[{}^3S_1^{(8)}] \rangle &= (2J + 1) \langle \mathcal{O}^{\chi_{c0}}[{}^3S_1^{(8)}] \rangle, \end{aligned} \quad (4)$$

which follow from heavy-quark spin symmetry in the LO in v . The color-singlet NMEs can be obtained from values of quarkonium radial wave function and its derivative in the origin by the following formulas:

$$\langle \mathcal{O}^{\mathcal{H}_J}[{}^3S_1^{(1)}] \rangle = 2N_c(2J + 1) \frac{1}{4\pi} |R(0)|^2, \quad (5)$$

$$\langle \mathcal{O}^{\mathcal{H}_J}[{}^3P_J^{(1)}] \rangle = 2N_c(2J + 1) \frac{3}{4\pi} |R'(0)|^2. \quad (6)$$

The partonic cross section of $b\bar{b}$ production is defined as

$$d\hat{\sigma}(R + R \rightarrow b\bar{b}[^{2S+1}L_J^{(1,8)}]) = \frac{1}{I} \overline{|\mathcal{A}(R + R \rightarrow b\bar{b}[^{2S+1}L_J^{(1,8)}])|^2} d\Phi, \quad (7)$$

where $I = 2x_1x_2S$ is the flux factor of the incoming particles, which is taken as in the collinear parton model [23], $\mathcal{A}(R + R \rightarrow b\bar{b}[^{2S+1}L_J^{(1,8)}])$ is the production amplitude, the overbar indicates average (summation) over initial-state (final-state) spins and colors, and $d\Phi$ is the invariant phase space volume of the outgoing particles. This convention implies that the cross section in the high-energy factorization scheme is normalized approximately to the cross section for on-shell gluons in the collinear parton model when $\mathbf{q}_{1T} = \mathbf{q}_{2T} = \mathbf{0}$.

Earlier we have found the LO results for the squared amplitudes of subprocesses (1) and (2) using the Feynman rules of Ref. [8]. The formulas for the squared amplitudes $\overline{|\mathcal{A}(R + R \rightarrow b\bar{b}[^{2S+1}L_J^{(1,8)}])|^2}$ for the $2 \rightarrow 1$ subprocesses (1) are listed in Eq. (27) of Ref. [18]. The analytical result in case of the $2 \rightarrow 2$ subprocess (2) is presented in Ref. [19].

Exploiting the hypothesis of high-energy factorization, we may write the hadronic cross section $d\sigma$ as a convolution of partonic cross section $d\hat{\sigma}$ with unintegrated parton distribution functions (PDFs) $\Phi_g^p(x, t, \mu^2)$ of Reggeized gluon in the proton, as

$$d\sigma(p + p \rightarrow \mathcal{H} + X) = \int \frac{dx_1}{x_1} \int \frac{d^2\mathbf{q}_{1T}}{\pi} \Phi_g^p(x_1, t_1, \mu^2) \int \frac{dx_2}{x_2} \int \frac{d^2\mathbf{q}_{2T}}{\pi} \times \Phi_g^p(x_2, t_2, \mu^2) d\hat{\sigma}(R + R \rightarrow \mathcal{H} + X). \quad (8)$$

$t_1 = |\mathbf{q}_{1T}|^2$, $t_2 = |\mathbf{q}_{2T}|^2$, x_1 and x_2 are the fractions of the proton momenta passed on to the Reggeized gluons, and the factorization scale μ is chosen to be of order M_T . The collinear and unintegrated gluon distribution functions are formally related as

$$xG^p(x, \mu^2) = \int^{\mu^2} \Phi_g^p(x, t, \mu^2) dt, \quad (9)$$

so that, for $\mathbf{q}_{1T} = \mathbf{q}_{2T} = \mathbf{0}$, we recover the conventional factorization formula of the collinear parton model,

$$d\sigma(p + p \rightarrow \mathcal{H} + X) = \int dx_1 G^p(x_1, \mu^2) \int dx_2 G^p(x_2, \mu^2) d\hat{\sigma}(g + g \rightarrow \mathcal{H} + X). \quad (10)$$

We now describe how to evaluate the differential hadronic cross section from Eq. (8) combined with the squared amplitudes of the $2 \rightarrow 1$ and $2 \rightarrow 2$ subprocesses (1) and (2), respectively. The rapidity and pseudorapidity of a bottomonium state with four-momentum $p^\mu = (p^0, \mathbf{p}_T, p^3)$ are defined as follows

$$y = \frac{1}{2} \ln \frac{p^0 + p^3}{p^0 - p^3}, \quad \eta = \frac{1}{2} \ln \frac{|\mathbf{p}| + p^3}{|\mathbf{p}| - p^3}. \quad (11)$$

In the following, we shall also use the shorthand notation $p_T = |\mathbf{p}_T|$ etc. for the absolute of the transverse two-momentum.

The master formula for the $2 \rightarrow 1$ subprocess (1) can be presented by the following way:

$$\frac{d\sigma(p + p \rightarrow \mathcal{H} + X)}{dp_T dy} = \frac{p_T}{(p_T^2 + M^2)^2} \int dt_1 \int d\varphi_1 \times \Phi_g^p(\xi_1, t_1, \mu^2) \Phi_g^p(\xi_2, t_2, \mu^2) |\overline{\mathcal{A}(R + R \rightarrow \mathcal{H})}|^2, \quad (12)$$

where $t_2 = t_1 + p_T^2 - 2p_T\sqrt{t_1} \cos(\phi_1)$, $\xi_1 = (p^0 + p^3)/\sqrt{S}$, $\xi_2 = (p^0 - p^3)/\sqrt{S}$ and the relation $\xi_1 \xi_2 S = M_T^2 = p_T^2 + M^2$ has been taken into account.

Than, we write the master formula for the $2 \rightarrow 2$ subprocess (2):

$$\frac{d\sigma(p + p \rightarrow \mathcal{H} + X)}{dp_T dy} = \frac{p_T}{(2\pi)^3} \int dt_1 \int d\varphi_1 \int dx_2 \int dt_2 \int d\varphi_2 \times \Phi_g^p(x_1, t_1, \mu^2) \Phi_g^p(x_2, t_2, \mu^2) \frac{|\overline{\mathcal{A}(R + R \rightarrow \mathcal{H} + g)}|^2}{(x_2 - \xi_2)(2x_1 x_2 S)^2}, \quad (13)$$

where $\phi_{1,2}$ are the angles enclosed between $\mathbf{q}_{1,2T}$ and the transverse momentum \mathbf{p}_T of \mathcal{H} ,

$$x_1 = \frac{1}{(x_2 - \xi_2)S} \left[(\mathbf{q}_{1T} + \mathbf{q}_{2T} - \mathbf{p}_T)^2 - M^2 - |\mathbf{p}_T|^2 + x_2 \xi_1 S \right]. \quad (14)$$

In our numerical analysis, we adopt as our default the prescription proposed by Kimber, Martin, and Ryskin (KMR) [24] to obtain unintegrated gluon PDF of the proton from the conventional integrated one, as implemented in Watt's code [25]. As input for these procedures, we use the LO set of the Martin-Roberts-Stirling-Thorne (MRST) [26] proton PDF as our default. Throughout our analysis the renormalization and factorization scales are identified and chosen to be $\mu = \xi M_T$, where ξ is varied between 1/2 and 2 about its default value 1 to estimate the theoretical uncertainty due to the freedom in the choice of scales. The resulting errors are indicated as shaded bands in the figures.

III. RESULTS

First of all, to extract the color-octet NMEs of the $\Upsilon(nS)$ -mesons, we perform a fit to the ATLAS Collaboration data [1] on prompt $\Upsilon(nS)$ -meson production collected in proton-proton collisions at the energy $\sqrt{S} = 7$ TeV in the two regions of rapidity $|y| < 1.2$ and $1.2 < |y| < 2.25$. This data set has the smallest statistical uncertainties and covers the largest interval in transverse momentum, namely $0 < p_T < 70$ GeV, in comparison with data sets from other CERN LHC collaborations. The $\Upsilon(3S)$ mesons are produced only directly via color-singlet and color-octet production mechanisms, $\Upsilon(1S)$ and $\Upsilon(2S)$ mesons are produced promptly, i.e. directly or through nonforbidden decays of higher-lying χ_{bJ} and $\Upsilon(nS)$ mesons, including cascade transitions such as $\Upsilon(3S) \rightarrow \chi_{b1} \rightarrow \Upsilon(1S)$. Notice that the contributions to prompt $\Upsilon(1S)$ and $\Upsilon(2S)$ production due to a feed-down are non-negligible for cascade decays up to the third order only. Thus, we introduce the matrix \hat{B} composed from the corresponding branching ratios of feed-down decays, which are extracted of the experimental data [27]. Then, the feed-down contribution can be evaluated as a product of the column-vector of direct cross sections and the matrix $\hat{B} + \hat{B}^2 + \hat{B}^3$. For the reader's convenience, we list the matrix \hat{B} in the Table I. Since the $\Upsilon(nS)$ mesons are identified through their decays to $\mu^+\mu^-$ pairs, we have to include the corresponding branching fractions, which we adopt from the recent Particle Data Group (PDG) report [27], $B(\Upsilon(1S) \rightarrow \mu^+\mu^-) = 0.0248$, $B(\Upsilon(2S) \rightarrow \mu^+\mu^-) = 0.0193$, and $B(\Upsilon(3S) \rightarrow \mu^+\mu^-) =$

0.0218.

Our fits of the color-octet NMEs include six experimental data samples, which come as p_T distributions of $\Upsilon(nS)$ mesons prompt production. In Table II we list our fit results, along with the values of color-singlet NMEs used. The last ones we determine by the equations (5, 6) using the quarkonium wave functions and their derivatives evaluated at the origin from potential models, see Ref. [28].

We perform a fit procedure with the positivity constraint on color-octet NMEs. Also, turning to the previous studies of charmonium and bottomonium production at the Fermilab Tevatron, we assume that $\chi_{b,J}$ mesons are produced directly only via the color-singlet mechanism, so we put the corresponding color-octet matrix elements equal to zero, see Table II.

The errors on the fit results are determined by varying in turn each NME up and down about its central value until the value of χ^2 is increased by unity keeping all other NMEs fixed at their central values. We found a quantity $\chi^2/d.o.f.$ to have a quite large value of 29.9. However, this result is foreseen, because in spite of the very small statistical and systematical errors of the ATLAS data, which were used for the χ^2 -procedure and indicated in the figures, in the region of $p_T < 10$ GeV these data contain a huge uncertainty due to polarization effects [1]. As the $\Upsilon(nS)$ production cross section is extracted from the inclusive $\mu^+\mu^-$ production cross section with the certain kinematical cuts, in the region of small p_T the result of such extraction is significantly dependent on the assumptions on polarization of produced quarkonium. The inclusion of this big uncertainty makes a fit too insensitive to the value of the cross section in the low- p_T region, so we decided to skip this uncertainty and increase the values of NMEs errors $\sqrt{\chi^2/d.o.f.}$ times, like it is implemented by the PDG in the cases of large values of $\chi^2/d.o.f.$ [27]. As it can be seen from Table II, the fit procedure strongly suppresses all color-octet NMEs except the $^3S_1^{(8)}$ NMEs for $\Upsilon(nS)$ mesons.

In Figs. 1–5, we compare our predictions obtained in the LO NRQCD and the parton Reggeization approach with the data on $\Upsilon(nS)$ mesons prompt production, measured by the ATLAS Collaboration (Fig. 1), by the CMS Collaboration (Fig. 2), by the LHCb Collaboration (Figs. 3–5), and by the CDF Collaboration (Fig. 6). It is important, the experimental data [1–3, 22] depend on the assumption of polarization of produced $\Upsilon(nS)$ mesons slightly. We perform our calculations and make a comparison to the data in a case of non-polarized $\Upsilon(nS)$ meson production.

Let us mention general features of $\Upsilon(nS)$ meson p_T distributions which are evident under all considered experimental conditions from LHC and Tevatron Colliders. The production of $\Upsilon(1S)$ and $\Upsilon(2S)$ mesons for $p_T < 20$ GeV and for all rapidities is dominated by the color-singlet mechanism while the color-octet production mechanism dominates only at large transverse momenta $p_T \geq 20$ GeV. This result confirms a naive estimation that at large transverse momentum the gluon fragmentation to bottomonium via gluon splitting to $b\bar{b}$ pair in the ${}^3S_1^{(8)}$ color-octet state should be more important. Roughly speaking, $\Upsilon(1S)$ prompt production can be described using color-singlet production mechanism only. It follows from the fact that a significant part of $\Upsilon(1S)$ mesons is produced directly through the color singlet mechanism or via cascade decays of higher-lying P -wave states χ_{Jb} .

The more important role of the color-octet mechanism appears in the production of $\Upsilon(3S)$ mesons. For the rapidities $|y| < 3$ its contribution amounts more than 50% of the cross section already from $p_T \geq 12$ GeV. This boundary rapidly decreases with growth of rapidity, and, as it follows from the comparison with LHCb data in Fig. 3, for the rapidities $|y| > 3$ the color-octet mechanism dominates at all values of p_T . In the region of large rapidities $|y| > 3.5$ shown in the Fig. 4, our model tends to overestimate the experimental cross section. The same feature was also observed in our study of charmonium production [20], and probably it reflects a violation of the QMRK condition at large values of $|y|$.

The P -wave bottomonium production in the parton Reggeization model can be described well in the color-singlet model, see Table I, as in the case of the P -wave charmonium production [18, 29]. In the Fig. 5, our prediction on the fraction of $\Upsilon(1S)$ mesons produced in the decays of $\chi_{bJ}(1P)$ mesons is compared with LHCb data [30]. We find a good agreement of this data with our prediction, despite the fact that this dataset was not included to the fit procedure. We predict additionally the fraction of $\Upsilon(2S)$ mesons produced in the decays of $\chi_{bJ}(2P)$ mesons.

In Fig. 6 one can find the CDF data [22] on prompt $\Upsilon(nS)$ production at $|y| < 0.4$ and $\sqrt{S} = 1.8$ TeV to be also well described by our model with the values of color-octet NMEs from Table II.

Comparing our results with the recent studies of $\Upsilon(nS)$ meson hadroproduction in the conventional collinear parton model performed in LO [32] and full NLO approximation of NRQCD formalism [33] or in the non-complete NNLO* approximation of color-singlet model [34], we should emphasize the following. Oppositely to the calculations in the collinear

parton model [32–34], we describe data at the small transverse momenta of $\Upsilon(nS)$ mesons (especially $\Upsilon(1S)$ meson) well, down to $p_T = 0$, at all values of rapidity. The LO heavy quarkonium production amplitudes in the parton Reggeization approach are finite at the $p_T = 0$ as well as the unintegrated gluon PDFs. Our predictions at the small $p_T < 10$ GeV have relatively large uncertainties, about factor 2, related with the strong dependence of cross section on the choice of the factorization scale μ . However, the central line corresponding to the default choice of $\mu = M_T$, lies rather close to the average values of the experimental data. The inclusion of small p_T region in a fit range is very important to separate different color-octet contributions and it changes the relative values of color-octet NMEs, comparing to the case when only large p_T region is taken into account.

The region of small p_T is also important to test the possibility of negative color-octet NMEs. This possibility was firstly supposed in [31], and it is used in modern full NLO studies of bottomonium production, such as Ref. [33]. To perform the fit of color-octet NMEs without the positivity condition (unconstrained fit), it is necessary to include into the fit as much experimental data as possible. The most important constraints on the values of color-octet NMEs are coming from the data on $\Upsilon(1S)$ fraction from the $\chi_{bJ}(1P)$ decays [30], and from the LHCb data at rapidities $|y| > 3$ [3]. In Ref. [33], also the data on $\Upsilon(1S)$ polarization were taken into account.

In our model, the unconstrained fit of the ATLAS data together with data on $\Upsilon(1S)$ fraction from the $\chi_{bJ}(1P)$ decays, significantly improves the description of experimental data at small rapidities, but leads to negative values of the cross section of $\Upsilon(3S)$ production for $p_T < 8$ GeV and $|y| > 3$. To avoid this problem, it is necessary to include LHCb data to the fit, which greatly suppresses the negative values of color-octet NMEs. So, we conclude that negative values of fit parameters are not necessary for the description of data at small values of p_T and large rapidities. Moreover, the positivity condition improves the predictive power of the model, allowing a reasonably good description of all present data on cross sections with just three free parameters.

Recently, the analysis of prompt $\Upsilon(nS)$ production at the LHC in view of the k_T -factorization approach was considered in Ref. [35]. Oppositely to our conclusions, it was found that data from CMS [2] and LHCb [3] Collaborations can be described using the color-singlet production mechanism only. Let us discuss here the main differences between our model and the model of Ref. [35].

In Ref. [35], it is suggested the occurrence of additional feed-down contribution from $\chi_{bJ}(3P)$ mesons, which is absent in our calculation. The first measurement of $\chi_{bJ}(3P)$ bottomonium state estimates its mass as $m(3P) = 10.530 \pm 0.014$ GeV [36]. This value is very close to the mass-threshold of open b -quark production, $m_{thr} = 2m(B^\pm) \simeq 10.558$ GeV, and $\chi_{bJ}(3P)$ meson seems as a very unstable state with unknown branching ratio $B(\chi_{bJ}(3P) \rightarrow \Upsilon(3S))$. We guess the inclusion of this contribution is still in dispute, moreover, it is non-negligible for the $\Upsilon(3S)$ meson spectra only.

Comparing the relative contributions of direct and feed-down production mechanisms, which are presented in Ref. [35], we see that a direct contribution dominates at small p_T and a feed-down contribution dominates at large values of p_T exceeding $5 - 7$ GeV. This result contradicts to the recent measurements of the LHCb Collaboration [30], which demonstrate that a fraction of $\Upsilon(1S)$ mesons from decays of $\chi_{bJ}(1P)$ mesons is approximately constant at all values of p_T (see Fig. 5), it is about 30 %. Such a way, in Ref. [35] the value of feed-down contribution to prompt $\Upsilon(nS)$ production is strongly overestimated, and in fact we need to take into account a color-octet production mechanism to describe the experimental data [1–3]. For precise comparison with results obtained in Ref. [35], we show in Fig. 7 our prediction for color-singlet contributions only. We see, the additional contribution is needed already at the $p_T \geq 10$ GeV and this contribution should have a gently sloping of the transverse momentum spectrum comparing to color-singlet contribution, that belongs only to the contribution of color-octet $^3S_1^{(8)}$ state, see Fig. 1 in Ref. [18].

We compare the results of our fit for color-octet NMEs with the values recently obtained in full NLO calculation of NRQCD approach [33]. If we take into account some differences between fit procedures used here and in Ref. [33] and perform a fit in a way of Ref. [33], we obtain the very similar values of color-octet NMEs for $^3S_1^{(8)}$ states. Such an agreement demonstrates a validity of factorization hypothesis in the bottomonium production in hadronic collisions, i.e. an independence of the $b\bar{b}$ production mechanism from the non-perturbative bottomonium formation at the last step. It is necessary to note, that a same consent between LO results obtained in the parton Reggeization approach and NLO results obtained in the collinear parton model is also observed describing charmonium production processes, see Refs. [18–20].

The present study along with the previous investigations in the parton Reggeization approach [9–15, 18–21] demonstrates the important role of (quasi)multi-Regge kinematics

in particle production at high energies, this feature is out of account in the collinear parton model. Such a way, we find the approach based on the effective theory of Reggeized partons [5, 6] and high-energy factorization scheme with unintegrated PDFs, in which the large logarithmic terms ($\ln(\mu^2/\Lambda_{QCD}^2)$, and $\ln(S/\mu^2)$) are resummed in all orders of strong coupling constant α_s , to be more adequate for the description of experimental data than fixed order calculations in α_s in the framework of collinear parton model.

IV. CONCLUSIONS

The CERN LHC is currently probing particle physics at terascale c.m. energies \sqrt{S} , so that the hierarchy $\Lambda_{QCD} \ll \mu \ll \sqrt{S}$, which defines the MRK and QMRK regimes, is satisfied for processes of heavy quark and heavy quarkonium production in the central region of rapidity, where μ is of order of their transverse mass. In this paper, we studied QCD processes of particular interest, namely prompt $\Upsilon(nS)$ hadroproduction, at LOs in the parton Reggeization approach and NRQCD approach, in which they are mediated by $2 \rightarrow 1$ and $2 \rightarrow 2$ partonic subprocesses initiated by Reggeized gluon collisions.

We found by the fit of ATLAS Collaboration data [1] the numerical values of the color-octet NMEs. Using these NMEs, we nicely describe recent LHC and old Tevatron data for prompt $\Upsilon(nS)$ meson production measured by ATLAS [1], CMS [2] and LHCb [3] Collaborations at the whole presented range of $\Upsilon(nS)$ transverse momenta and rapidity y . Here and in Refs. [9–15, 18–21], the parton Reggeization approach was demonstrated to be a powerful tool for the theoretical description of QCD processes in the high-energy limit.

V. ACKNOWLEDGEMENTS

We are grateful to B. A. Kniehl and N. N. Nikolaev for useful discussions. The work of V. S. was supported by the Ministry for Science and Education of the Russian Federation under Contract No. 2.870.2011. The work of M. N. and A. S. was supported in part by the Russian Foundation for Basic Research under Grant 12-02-31701-mol-a. The work of M. N. is supported also by the Grant of the Graduate Students Stipend Program of the Dynasty Foundation.

-
- [1] ATLAS Collaboration, G. Aad et al. Phys. Rev. D **87**, 052004 (2013).
- [2] CMS Collaboration, S. Chatrchyan et al. Phys. Rev. D **83**, 112004 (2011).
- [3] LHCb Collaboration, R. Aaij et al. Eur. Phys. J. **C72**, 2025 (2012).
- [4] V. S. Fadin and L. N. Lipatov, Nucl. Phys. **B406**, 259 (1993); **B477**, 767 (1996).
- [5] L. N. Lipatov, Nucl. Phys. **B452**, 369 (1995).
- [6] L. N. Lipatov, Sov. J. Nucl. Phys. **23**, 338 (1976) [Yad. Fiz. **23**, 642 (1976)]; E. A. Kuraev, L. N. Lipatov, and V. S. Fadin, Sov. Phys. JETP **44**, 443 (1976) [Zh. Eksp. Teor. Fiz. **71**, 840 (1976)]; Sov. Phys. JETP **45**, 199 (1977) [Zh. Eksp. Teor. Fiz. **72**, 377 (1977)]; I. I. Balitsky and L. N. Lipatov, Sov. J. Nucl. Phys. **28**, 822 (1978) [Yad. Fiz. **28**, 1597 (1978)]; Sov. Phys. JETP **63**, 904 (1986) [Zh. Eksp. Teor. Fiz. **90**, 1536 (1986)].
- [7] L. N. Lipatov and M. I. Vyazovsky, Nucl. Phys. **B597**, 399 (2001).
- [8] E. N. Antonov, L. N. Lipatov, E. A. Kuraev, and I. O. Cherednikov, Nucl. Phys. **B721**, 111 (2005).
- [9] B. A. Kniehl, V. A. Saleev, A. V. Shipilova, E. V. Yatsenko, Phys. Rev. **D84**, 074017 (2011).
- [10] M.A. Nefedov, V.A. Saleev, A.V. Shipilova, Preprint DESY-13-070 [arXiv:1304.3549[hep-ph]].
- [11] V. A. Saleev, Phys. Rev. D **78**, 034033 (2008); Phys. Rev. D **78**, 114031 (2008).
- [12] V. A. Saleev, Phys. Rev. D **80**, 114016 (2009).
- [13] B. A. Kniehl, A. V. Shipilova, and V. A. Saleev, Phys. Rev. D **79**, 034007 (2009).
- [14] B. A. Kniehl, V. A. Saleev, and A. V. Shipilova, Phys. Rev. D **81**, 094010 (2010) [arXiv:1003.0346 [hep-ph]]; V.A. Saleev and A.V. Shipilova, Phys. Rev. D **86**, 034032 (2012).
- [15] M.A. Nefedov, N.N. Nikolaev, and V.A. Saleev, Phys. Rev. D **87**, 014022 (2013).
- [16] G. T. Bodwin, E. Braaten, and G. P. Lepage, Phys. Rev. D **51**, 1125 (1995); **55**, 5853(E) (1997).
- [17] F. Maltoni, M. L. Mangano, and A. Petrelli, Nucl. Phys. **B519**, 361 (1998).
- [18] B. A. Kniehl, D. V. Vasin, and V. A. Saleev, Phys. Rev. D **73**, 074022 (2006).
- [19] D. V. Vasin, V. A. Saleev, Phys. Part. Nucl. **38**, 635-658 (2007).
- [20] V.A. Saleev, M.A. Nefedov, and A.V. Shipilova, Phys. Rev. D **85**, 074013 (2012).
- [21] B. A. Kniehl, V. A. Saleev, and D. V. Vasin, Phys. Rev. D **74**, 014024 (2006).
- [22] CDF Collaboration, F. Abe et al., Phys. Rev. Lett. **75**, 4358 (1995); D. Acosta et al., Phys.

- Rev. Lett. **88**, 161802 (2002); V.M. Abazov et al., Phys. Rev. Lett. **94**, 232001 (2005).
- [23] J. C. Collins and R. K. Ellis, Nucl. Phys. **B360**, 3 (1991).
- [24] M. A. Kimber, A. D. Martin, and M. G. Ryskin, Eur. Phys. J. C **12**, 655 (2000); Phys. Rev. D **63**, 114027 (2001); G. Watt, A. D. Martin, and M. G. Ryskin, Eur. Phys. J. C **31**, 73 (2003); Phys. Rev. D **70**, 014012 (2004); **70**, 079902(E) (2004).
- [25] G. Watt, URL: <http://gwatt.web.cern.ch/gwatt/>.
- [26] A. D. Martin, R. G. Roberts, W. J. Stirling, and R. S. Thorne, Phys. Lett. B **531**, 216 (2002); A. D. Martin, W. J. Stirling, and R. S. Thorne, Phys. Lett. **B636** (2006) 259-264.
- [27] J. Beringer et. al. (Particle Data Group), Phys. Rev. D **86**, 010001 (2012).
- [28] E. J. Eichten, C. Quigg, Phys. Rev. D **52**, 1726 (1995).
- [29] Ph. Hagler, R. Kirschner, A. Schafer, L. Szymanowski, and O. V. Teryaev, Phys. Rev. D **63**, 077501 (2001); Phys. Rev. Lett. **86**, 1446 (2001).
- [30] LHCb Collaboration, R. Aaij et al. J. High Energy Phys. **11** 031 (2012)
- [31] M. Butenschoen, B. A. Kniehl, Phys. Rev. D **84** 051501 (2011)
- [32] E. Braaten, S. Fleming, and A.K. Leibovich, Phys. Rev. D **63**, 094006 (2001); E. Braaten, and J. Lee, Phys. Rev. D **63**, 071501 (2001).
- [33] B. Gong, J.-X. Wang, and H.-F. Zhang, Phys. Rev. D **83**, 114021 (2011); K. Wang, Y.-Q. Ma, and K.-T.Chao, Phys. Rev. D **85**, 114003 (2012); B. Gong, L.-P. Wan, J.-X. Wang, and H.-F. Zhang, E-print [arXiv:1305.0748 [hep-ph]] (2013).
- [34] P. Artoisenet et al. Phys. Rev. Lett. **101**, 152001 (2008); J. P. Lansberg, Phys. Lett. B **695**, 149 (2011).
- [35] S.P. Baranov, Phys. Rev. D **86**, 054015 (2012).
- [36] G. Aad et al. ATLAS Collaboration, Phys. Rev. Lett. **108**, 152001 (2012).

TABLE I: Matrix of the inclusive branching fractions. All known branchings are taken from [27], others are supposed to be equal to zero.

Out \ In	$\Upsilon(3S)$	$\chi_{b2}(2P)$	$\chi_{b1}(2P)$	$\chi_{b0}(2P)$	$\Upsilon(2S)$	$\chi_{b2}(1P)$	$\chi_{b1}(1P)$	$\chi_{b0}(1P)$
$\chi_{b2}(2P)$	0.131	–	–	–	–	–	–	–
$\chi_{b1}(2P)$	0.126	–	–	–	–	–	–	–
$\chi_{b0}(2P)$	0.059	–	–	–	–	–	–	–
$\Upsilon(2S)$	0.106	0.106	0.199	0.046	–	–	–	–
$\chi_{b2}(1P)$	0.0099	0.0051	–	–	0.0715	–	–	–
$\chi_{b1}(1P)$	0.0009	–	0.0091	–	0.069	–	–	–
$\chi_{b0}(1P)$	0.0027	–	–	–	0.0038	–	–	–
$\Upsilon(1S)$	0.0657	0.081	0.108	0.009	0.2652	0.191	0.339	0.0176

TABLE II: The color-singlet and color-octet NMEs used in the calculation.

NME	Fit in LO of parton Reggeization approach.
$\langle \mathcal{O}^{\Upsilon(1S)} [{}^3S_1^{(1)}] \rangle \times \text{GeV}^{-3}$	9.28
$\langle \mathcal{O}^{\Upsilon(1S)} [{}^3S_1^{(8)}] \rangle \times 10^2 \text{ GeV}^{-3}$	2.31 ± 0.25
$\langle \mathcal{O}^{\Upsilon(1S)} [{}^1S_0^{(8)}] \rangle \times 10^2 \text{ GeV}^{-3}$	0.0 ± 0.05
$\langle \mathcal{O}^{\Upsilon(1S)} [{}^3P_0^{(8)}] \rangle \times 10^2 \text{ GeV}^{-5}$	0.0 ± 0.38
$\langle \mathcal{O}^{\Upsilon(2S)} [{}^3S_1^{(1)}] \rangle \times \text{GeV}^{-3}$	4.62
$\langle \mathcal{O}^{\Upsilon(2S)} [{}^3S_1^{(8)}] \rangle \times 10^2 \text{ GeV}^{-3}$	1.51 ± 0.17
$\langle \mathcal{O}^{\Upsilon(2S)} [{}^1S_0^{(8)}] \rangle \times 10^2 \text{ GeV}^{-3}$	0.0 ± 0.01
$\langle \mathcal{O}^{\Upsilon(2S)} [{}^3P_0^{(8)}] \rangle \times 10^2 \text{ GeV}^{-5}$	0.0 ± 0.03
$\langle \mathcal{O}^{\Upsilon(3S)} [{}^3S_1^{(1)}] \rangle \times \text{GeV}^{-3}$	3.54
$\langle \mathcal{O}^{\Upsilon(3S)} [{}^3S_1^{(8)}] \rangle \times 10^2 \text{ GeV}^{-3}$	1.24 ± 0.13
$\langle \mathcal{O}^{\Upsilon(3S)} [{}^1S_0^{(8)}] \rangle \times 10^2 \text{ GeV}^{-3}$	0.0 ± 0.01
$\langle \mathcal{O}^{\Upsilon(3S)} [{}^3P_0^{(8)}] \rangle \times 10^2 \text{ GeV}^{-5}$	0.0 ± 0.02
$\langle \mathcal{O}^{\chi(1P)} [{}^3P_0^{(1)}] \rangle \times \text{GeV}^{-5}$	2.03
$\langle \mathcal{O}^{\chi(1P)} [{}^3S_1^{(8)}] \rangle \times 10^2 \text{ GeV}^{-3}$	0.0
$\langle \mathcal{O}^{\chi(2P)} [{}^3P_0^{(1)}] \rangle \times \text{GeV}^{-5}$	2.36
$\langle \mathcal{O}^{\chi(2P)} [{}^3S_1^{(8)}] \rangle \times 10^2 \text{ GeV}^{-3}$	0.0

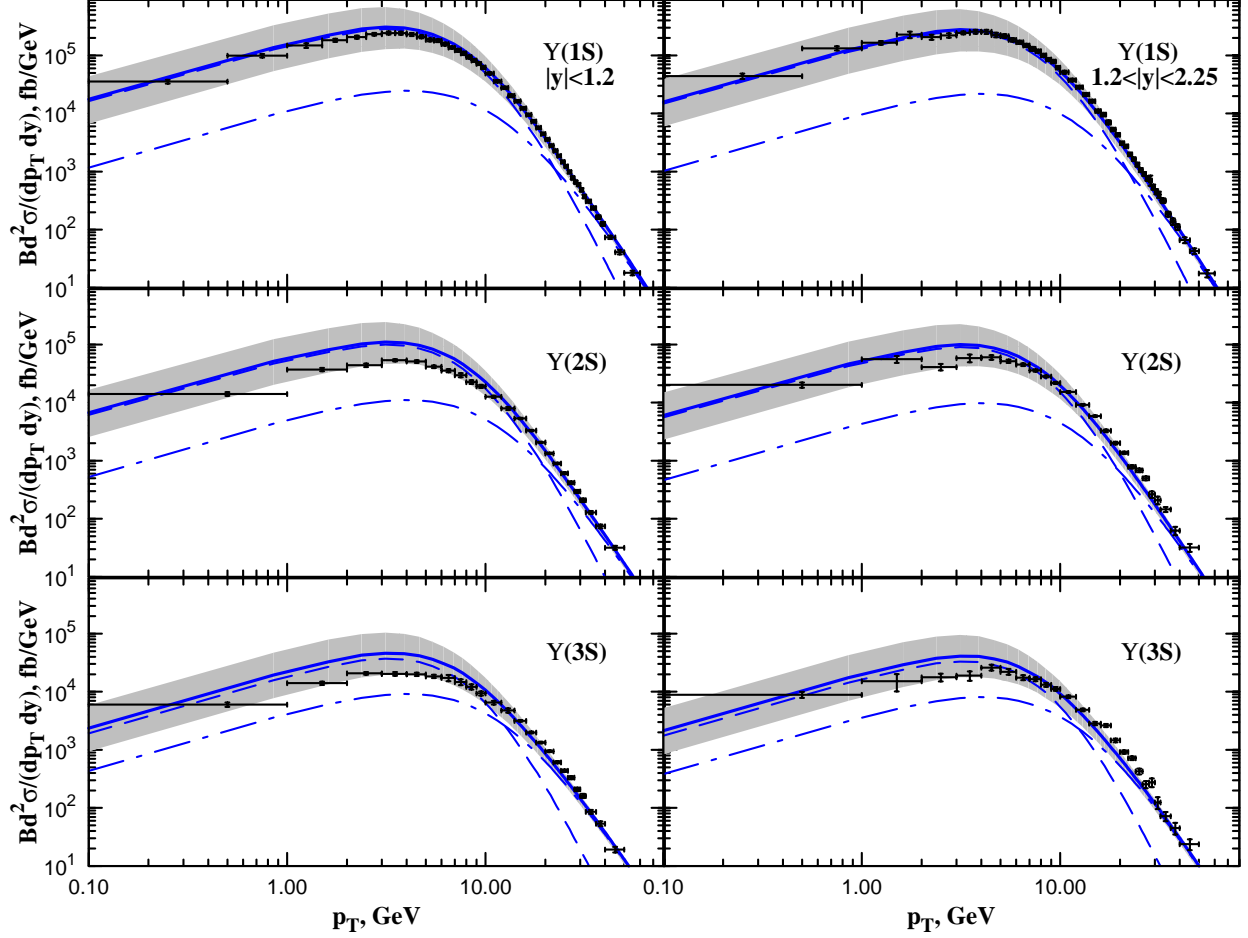


FIG. 1: Transverse momentum distributions of prompt $\Upsilon(1S)$, $\Upsilon(2S)$, and $\Upsilon(3S)$ hadroproduction in pp scattering with $\sqrt{S} = 7$ TeV and $|y| < 1.2$ (left panel) and $1.2 < |y| < 2.25$ (right panel), including the respective decay branching fractions $B(\Upsilon(nS) \rightarrow \mu^+\mu^-)$. The data are from the ATLAS Collaboration [1]. The curves correspond to LO of NRQCD and parton Reggeization approach: dashed line is the color-singlet contribution, dash-dotted line is the color-octet contribution, solid line is their sum.

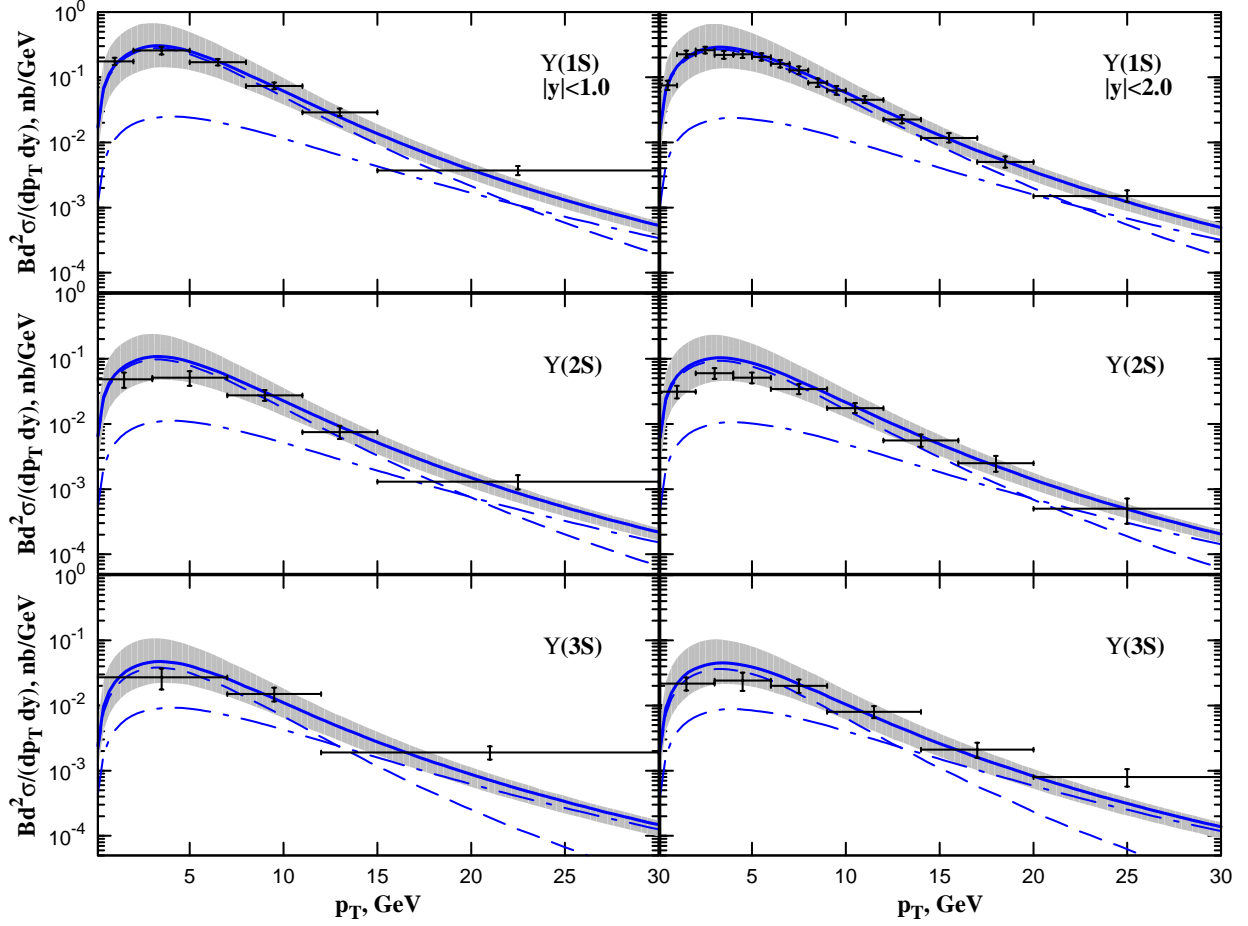


FIG. 2: Transverse momentum distributions of prompt $\Upsilon(1S)$, $\Upsilon(2S)$, and $\Upsilon(3S)$ hadroproduction in pp scattering with $\sqrt{S} = 7$ TeV and $|y| < 1.0$ (left panel) and $|y| < 2.0$ (right panel), including the respective decay branching fractions $B(\Upsilon(nS) \rightarrow \mu^+\mu^-)$. The data are from the CMS Collaboration [2]. The curves are the same as in the Fig. 1.

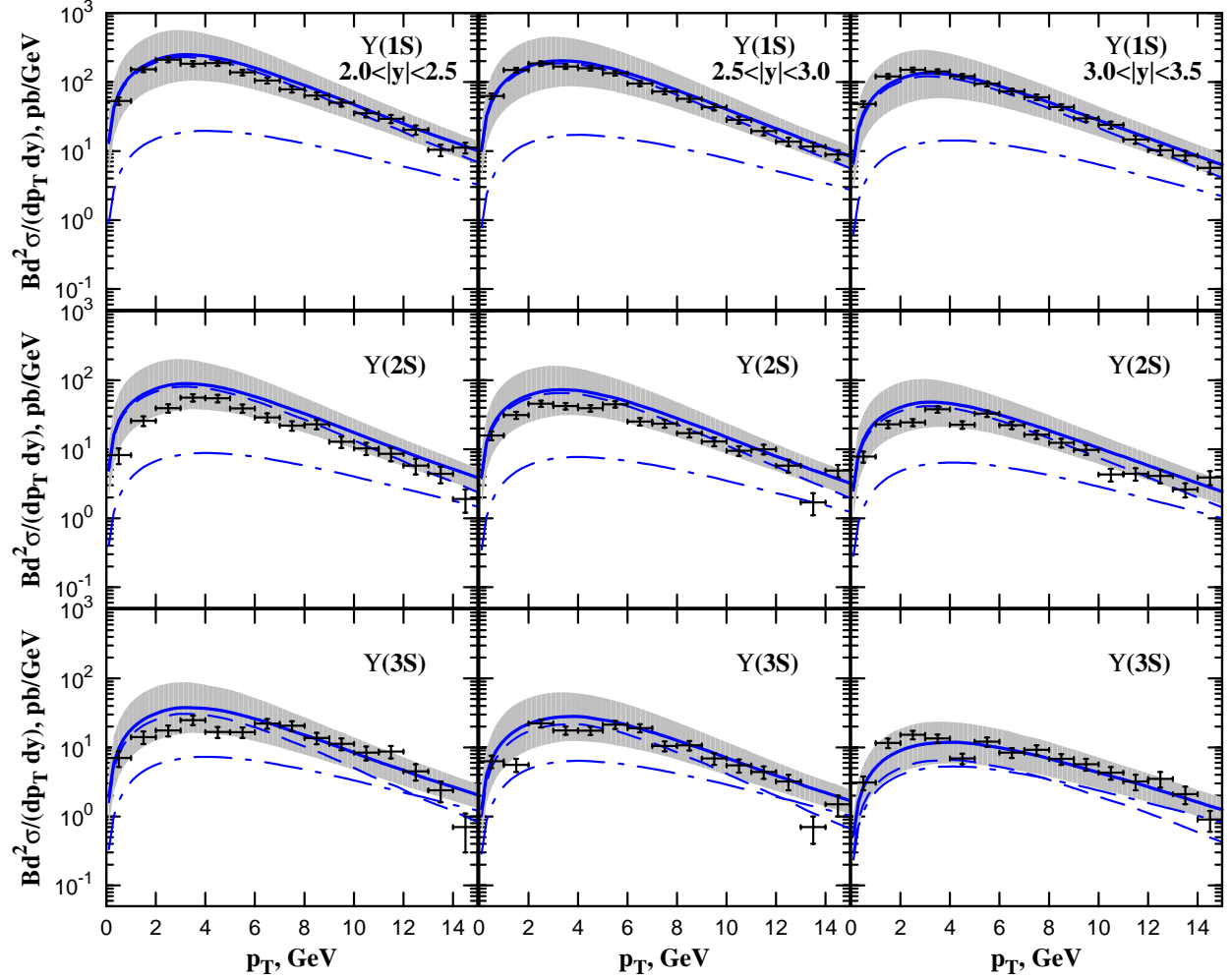


FIG. 3: Transverse momentum distributions of prompt $\Upsilon(1S)$, $\Upsilon(2S)$, and $\Upsilon(3S)$ hadroproduction in pp scattering with $\sqrt{S} = 7$ TeV and $2.0 < |y| < 2.5$ (left panel), $2.5 < |y| < 3.0$ (central panel), and $3.0 < |y| < 3.5$ (right panel), including the respective decay branching fractions $B(\Upsilon(nS) \rightarrow \mu^+\mu^-)$. The data are from the LHCb Collaboration [3]. The curves are the same as in the Fig. 1.

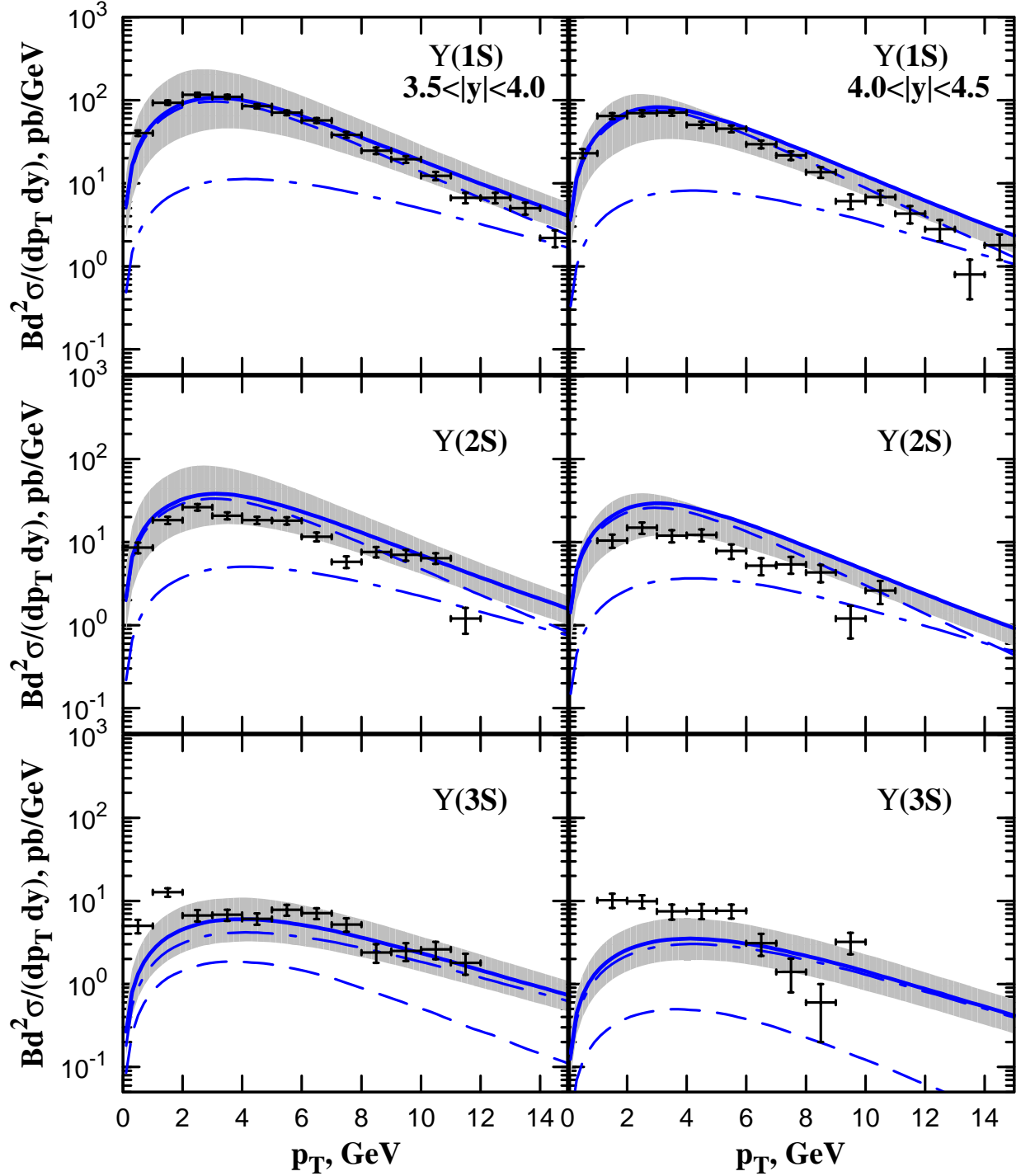


FIG. 4: Transverse momentum distributions of prompt $\Upsilon(1S)$, $\Upsilon(2S)$, and $\Upsilon(3S)$ hadroproduction in pp scattering with $\sqrt{S} = 7$ TeV and $3.5 < |y| < 4.0$ (left panel), and $4.0 < |y| < 4.5$ (right panel), including the respective decay branching fractions $B(\Upsilon(nS) \rightarrow \mu^+\mu^-)$. The data are from the LHCb Collaboration [3]. The curves are the same as in the Fig. 1.

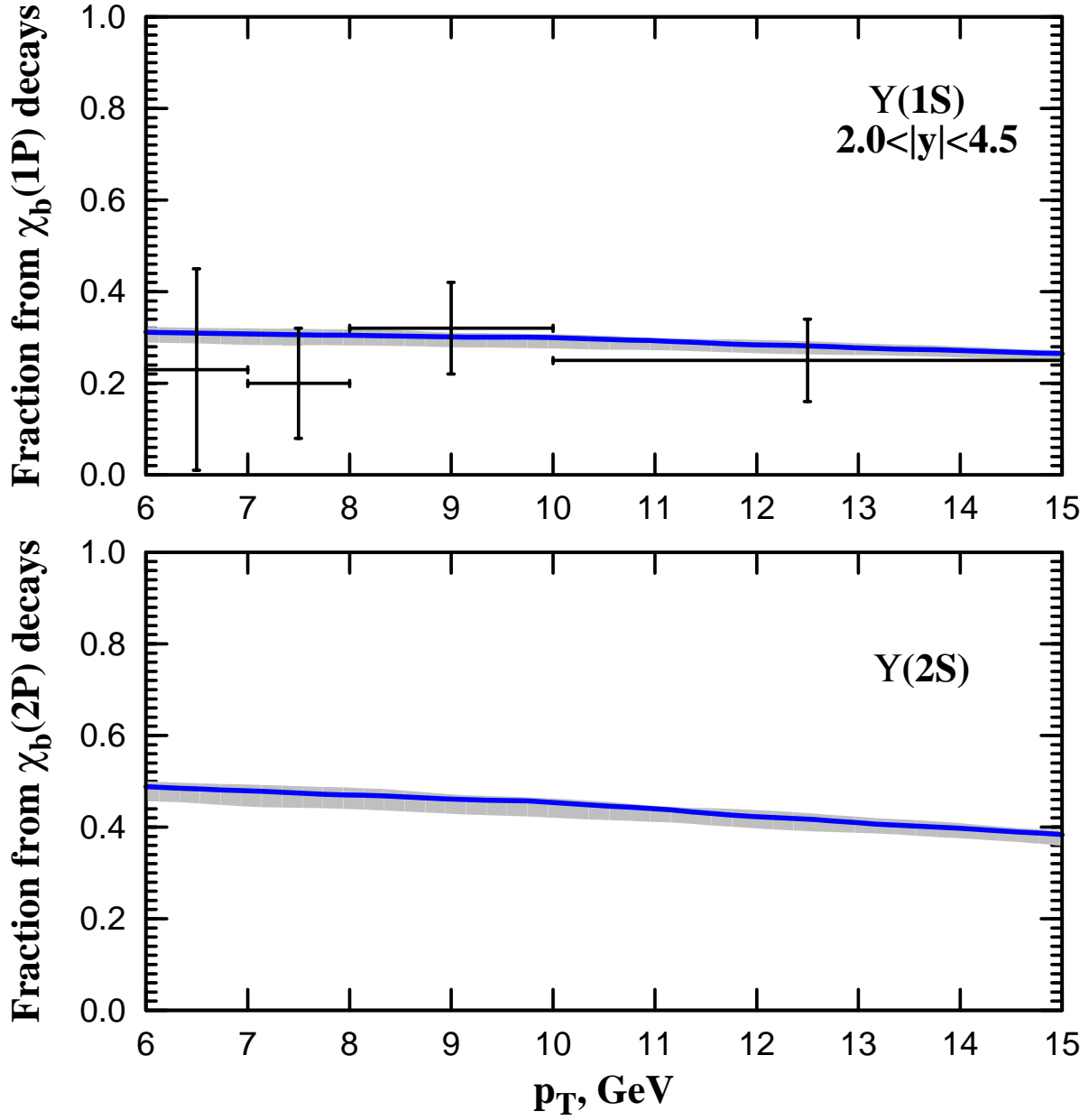


FIG. 5: Transverse momentum distributions of $\Upsilon(1S)$ fraction producing via $\chi_b(1P)$ decays in pp scattering with $\sqrt{S} = 7$ TeV and $2.0 < |y| < 4.5$. The data are from the LHCb Collaboration [3].

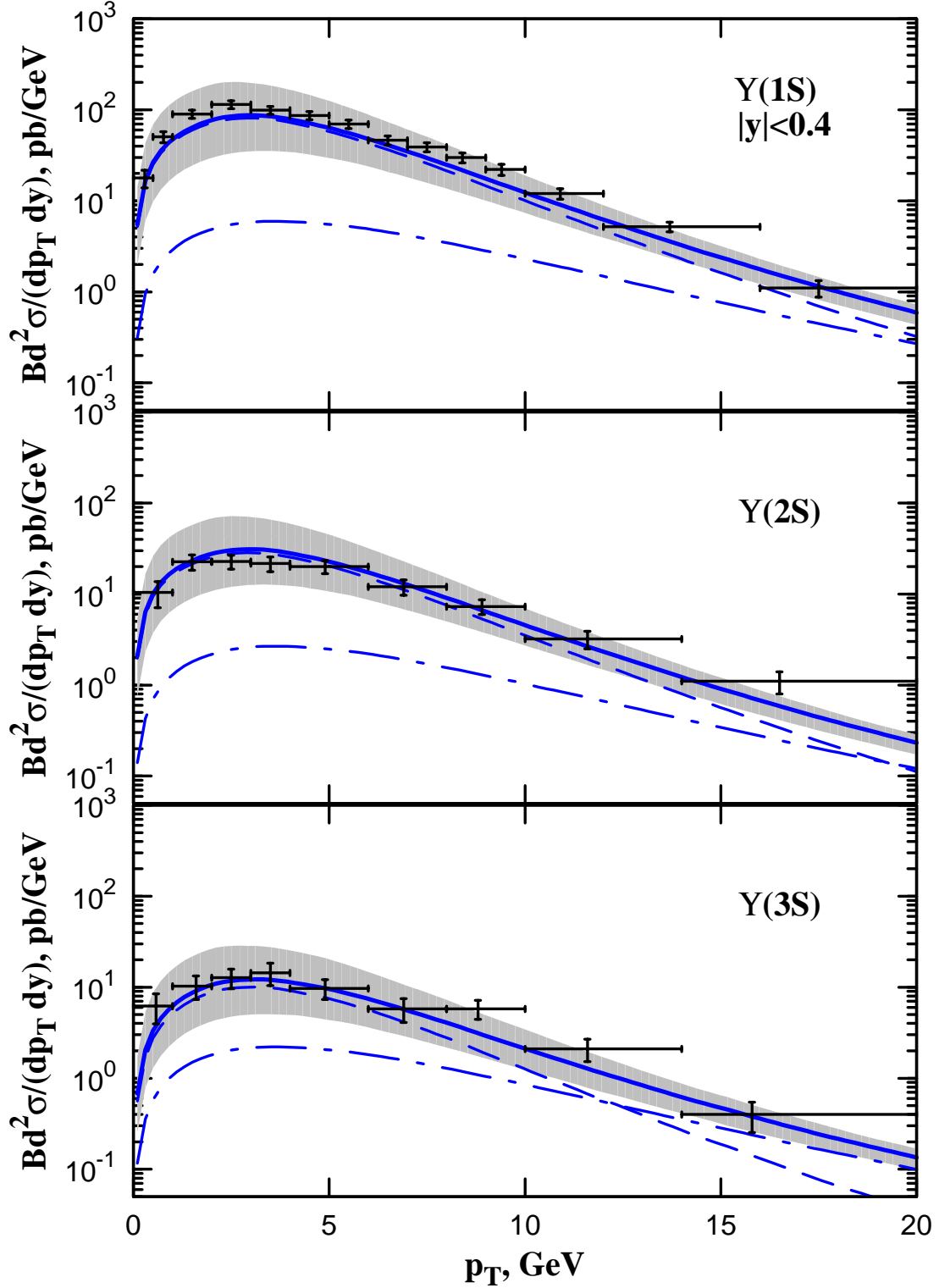


FIG. 6: Transverse momentum distributions of prompt $\Upsilon(1S)$, $\Upsilon(2S)$, and $\Upsilon(3S)$ hadroproduction in pp scattering with $\sqrt{S} = 7$ TeV and $|y| < 0.4$, including the respective decay branching fractions $B(\Upsilon(nS) \rightarrow \mu^+\mu^-)$. The data are from the CDF Collaboration [22]. The curves are the same as in the Fig. 1.

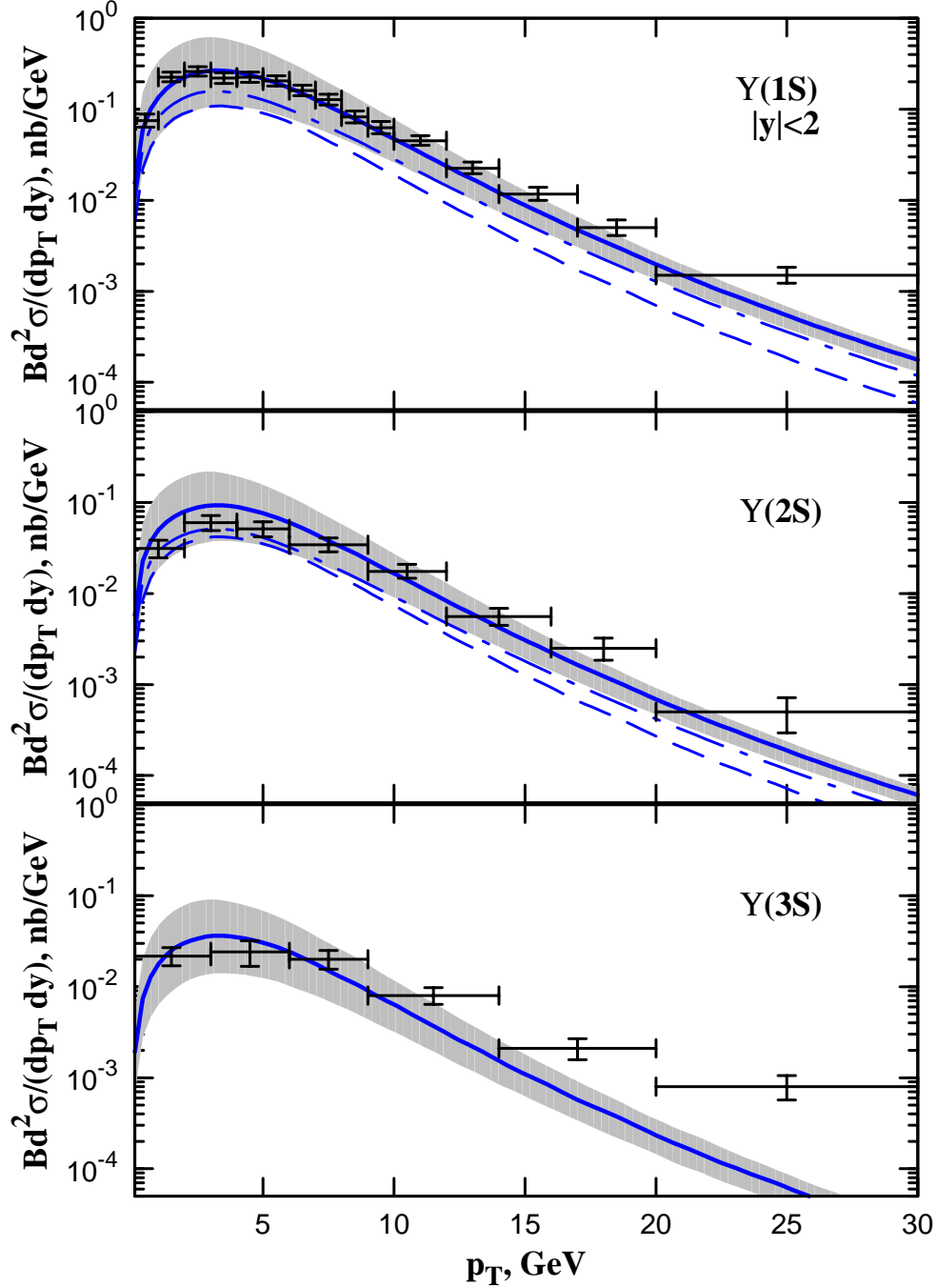


FIG. 7: Transverse momentum distributions of prompt $\Upsilon(1S)$, $\Upsilon(2S)$, and $\Upsilon(3S)$ hadroproduction in pp scattering with $\sqrt{S} = 7$ TeV and $|y| < 2$, including the respective decay branching fractions $B(\Upsilon(nS) \rightarrow \mu^+\mu^-)$. The data are from the CMS Collaboration [2]. The curves correspond to LO of color-singlet model and parton Reggeization approach: dashed line is the direct contribution, dash-dotted line is the feed-down contribution, solid line is their sum.